

Video Article

Deep Brain Stimulation with Simultaneous fMRI in Rodents

John Robert Younce^{1,2,5}, Daniel L Albaugh^{1,2,4}, Yen-Yu Ian Shih^{1,2,3,4}¹Department of Neurology, University of North Carolina²Biomedical Research Imaging Center, University of North Carolina³Department of Biomedical Engineering, University of North Carolina⁴Curriculum in Neurobiology, University of North Carolina⁵School of Medicine, University of North CarolinaCorrespondence to: Yen-Yu Ian Shih at shihy@neurology.unc.eduURL: <http://www.jove.com/video/51271>DOI: [doi:10.3791/51271](https://doi.org/10.3791/51271)

Keywords: Neuroscience, Issue 84, Electric Stimulation Therapy, Animal Experimentation, Immobilization, Intubation, Models, Animal, Neuroimaging, Functional Neuroimaging, Stereotaxic Techniques, Functional magnetic resonance imaging (fMRI), deep brain stimulation (DBS), blood oxygen level dependent (BOLD), subthalamic nucleus, rodent

Date Published: 2/15/2014

Citation: Younce, J.R., Albaugh, D.L., Shih, Y.Y.I. Deep Brain Stimulation with Simultaneous fMRI in Rodents. *J. Vis. Exp.* (84), e51271, doi:10.3791/51271 (2014).

Abstract

In order to visualize the global and downstream neuronal responses to deep brain stimulation (DBS) at various targets, we have developed a protocol for using blood oxygen level dependent (BOLD) functional magnetic resonance imaging (fMRI) to image rodents with simultaneous DBS. DBS fMRI presents a number of technical challenges, including accuracy of electrode implantation, MR artifacts created by the electrode, choice of anesthesia and paralytic to minimize any neuronal effects while simultaneously eliminating animal motion, and maintenance of physiological parameters, deviation from which can confound the BOLD signal. Our laboratory has developed a set of procedures that are capable of overcoming most of these possible issues. For electrical stimulation, a homemade tungsten bipolar microelectrode is used, inserted stereotactically at the stimulation site in the anesthetized subject. In preparation for imaging, rodents are fixed on a plastic headpiece and transferred to the magnet bore. For sedation and paralysis during scanning, a cocktail of dexmedetomidine and pancuronium is continuously infused, along with a minimal dose of isoflurane; this preparation minimizes the BOLD ceiling effect of volatile anesthetics. In this example experiment, stimulation of the subthalamic nucleus (STN) produces BOLD responses which are observed primarily in ipsilateral cortical regions, centered in motor cortex. Simultaneous DBS and fMRI allows the unambiguous modulation of neural circuits dependent on stimulation location and stimulation parameters, and permits observation of neuronal modulations free of regional bias. This technique may be used to explore the downstream effects of modulating neural circuitry at nearly any brain region, with implications for both experimental and clinical DBS.

Video Link

The video component of this article can be found at <http://www.jove.com/video/51271/>

Introduction

Determining the global downstream effects of neural circuit activity represents a major challenge and goal for many areas of systems neuroscience. A paucity of tools are currently available that meet this need, and thus there is a demand for increased accessibility of the appropriate experimental setups. One such method for evaluating the global consequence of neural circuit activation relies on the simultaneous application of deep brain electrical stimulation (DBS) and functional MRI (fMRI). DBS-fMRI allows for the detection of downstream responses to circuit activation on a large spatial scale, and can be applied at virtually any stimulation target. This toolset is highly suitable for translational preclinical studies, including the characterization of responses to therapeutic high frequency stimulation.

In addition to access to a suitable MRI scanner, successful DBS-fMRI experiments require consideration of a number of variables, including electrode type, sedation method, and maintenance of physiological parameters. For example, electrode choice should be based on factors relating to stimulation efficacy (e.g. lead size and conductance, mono- vs. bipolar), as well as MR compatibility and electrode artifact size. Electrode artifacts vary according to electrode material and size, as well as the scan sequence used; thorough pre-experimental testing should be employed to determine the appropriate electrode type for each study. In general, tungsten microwire electrodes are recommended for this protocol. Choice of paralytic and sedative should be made to effectively immobilize the animal and reduce the suppressive effects of certain sedatives on blood-oxygen-level-dependent (BOLD) signal. Lastly, it is critical to maintain the animal at optimal physiological parameters, including body temperature and oxygen saturation.

The protocol that we have developed for DBS-fMRI overcomes many of these potential obstacles, and in our hands, provides robust and consistent results. Additionally, these experimental procedures may be readily adopted for the combination of fMRI with alternative stimulation methods, including optogenetic stimulation.

Protocol

Ethics Statement: This procedure is in accordance with the National Institutes of Health Guidelines for Animal Research (Guide for the Care and Use of Laboratory Animals) and is approved by the University of North Carolina Institutional Animal Care and Use Committee.

1. Electrode Implantation

The first step is electrode implantation. In this step, an electrode is unilaterally implanted into the subthalamic nucleus (STN), a small nucleus with translational significance for Parkinson's disease treatment using the following methods:

1. Sterilize all surgical equipment using an autoclave, or antiseptic solution where autoclaving is not possible (e.g. for electrode sterility). **Note:** this is a short-term survival surgery, and thus aseptic technique is essential. Following surgery, animals can be imaged after a brief recovery period (48 hr) or up to several weeks later.
2. Anesthetize the rat (Adult Sprague-Dawley rats 250-400 g) using 2.5% isoflurane administered via endotracheal intubation and a small animal ventilator. Fix the rat to a stereotactic surgical frame and prepare the surgical site using aseptic techniques.
3. Prepare and ensure that the electrode is sterile. A homemade 2-channel tungsten microwire electrode is used for this procedure, though many MRI-compatible electrode types will work. The electrode type used may affect the area of tissue mechanically damaged by the procedure, the area of tissue stimulated, and the accuracy of implantation, thus affecting the overall experimental result. If the electrode type is not able to be autoclaved, use povidone-iodine antiseptic to sterilize the electrode as far as is possible.
4. Using scissors remove the scalp over the site of implantation with a diameter of approximately 1.5 cm, to uncover bregma and lambda on the skull. Remove the muscle and fascia overlying the skull and stop all bleeding using electrocautery.
5. Scratch the skull surface in multiple directions with a scalpel to improve dental cement adhesion (step 1.8). Level Bregma and Lambda in the horizontal direction.
6. To target STN, at 3.6 mm posterior to Bregma and 2.5 mm lateral to midline, use a small-tipped electric drill to create a burr hole measuring approximately 1.5 mm in diameter. **Note:** The exact location of the STN in reference to stereotaxic coordinates may vary by rat strain, weight, and gender. Adult rats of the same gender should be used to minimize any variation in location. If possible, pre-operational anatomical scans or intraoperative electrical recordings should be used to identify the STN location on an individual subject basis. Further, electrode termination sites should be histologically verified to ensure target accuracy.
 1. Carefully make an incision in the dura, and use small blunt forceps to move the dura to the sides of the hole. Stop any bleeding using sterile cotton soaked in saline. Create holes for one or more MR-compatible screws) and insert them gently in the skull until they are stable. Screws may be placed in any location where they will not disrupt the placement of the external connector for the DBS electrode (e.g. not directly behind the STN ipsilateral to the electrode). We recommend placements at the lateral edges of the skull, ideally directly posterior to the lambda suture. At this point, the skull is relatively thick, reducing the likelihood that screws will damage the cortex." **Note:** Brass screws cut to 4-5 mm in length are used in this protocol, although plastic screws are also suitable.
7. Place the electrode on the stereotactic arm, ensuring that it is straight and vertical. Touch the electrode to Bregma, then move the electrode exactly 3.6 mm posterior to Bregma and 2.5 mm lateral to midline and touch the cortical surface with the electrode. From the cortical surface, insert the electrode 7.8 mm ventrally. These coordinates are determined by reference to a neuroanatomical atlas¹.
8. Place a layer of dental cement over the skull including the skull screws and electrode insertion point. Wait until the cement is completely hardened prior to removing the electrode from the stereotactic frame. Bend the electrode backward and use additional cement to cover the rest of the electrode tract and connector for durability.

2. fMRI Preparation

The second step is the setup for fMRI, including positioning of the coil and setup of physiological monitoring equipment.

1. Secure the animal's head to prevent motion during the scan. **Note:** A custom plastic intraauricular bar system is used here for head fixation. Place the bars into the ear canals and secure to the headpiece so that the head rotates smoothly in the vertical direction with no horizontal rotation. Secure the head position by fixing the upper teeth to the apparatus.
2. Anesthetize the rat completely and monitor end tidal CO₂ to ensure stability throughout all scans. To maintain anesthesia, ventilation and control end tidal CO₂ levels during the scan, an MR-compatible small animal ventilation system combined with an isoflurane vaporizer is used here, though a variety of anesthetic and sedation agents may be used in a similar fashion. Set the ventilator to 45 breaths/min with a moderate volume, approximately 500 ml/min of air as a starting volume. Set the isoflurane to 2% and transfer the rat into the scan room. Attach the ventilator's output to the rat's endotracheal tube and press firmly to secure. Capnometry should be acquired using a tube connected as closely to the endotracheal tube connector as possible. Adjust ventilation volume to produce an end-tidal CO₂ of 2.6% to 3.3%.
3. Use an MR-compatible small animal holder to insert the rat into the scanner with a circulating hot water bath for temperature control. Tape the pad of the bath onto the holder and cover it with clean absorbent paper. Place the rat onto the hot water bed.
4. Monitoring of temperature and carbon dioxide levels are essential to BOLD fMRI, while arterial oxygen saturation and heart rate are also useful physiological parameters. Insert an MR-compatible rectal temperature probe and tape it to the base of the tail, and then adjust the temperature of the water bath to maintain normal body temperature at 37 °C. Monitor arterial oxygen saturation and heart rate using a small animal pulse oximetry system, maintaining them at 95-98% and 250-350 bpm, respectively, which may vary depending on the type of anesthetics used. Oxygen saturation and heart rate are both influenced by depth of anesthesia, ventilation volume and ventilation rate. Ventilation volume and rate may need to be carefully balanced to maintain adequate end-tidal CO₂ levels and adequate oxygen saturation.
5. A surface coil is needed for BOLD fMRI acquisition. Place the surface coil as close to the surface of the head as possible. Once secured, place toothpaste on the surface of the head on the cement cap in order to reduce susceptibility artifacts near the brain surface. **Note:** We use a homemade transceiver surface coil with an internal diameter of approximately 1.6 cm, though larger surface coils may be used to optimize the BOLD response in deeper subcortical regions.

6. Connect the stimulating electrode to a programmable electrical stimulator system. **Note:** We use a custom-made programmable TTL triggering system connected to a bipolar stimulator to deliver electrical pulses synchronized to the RF excitations from the MR scans.
7. For sedation and paralysis during fMRI data acquisition, use a cocktail of dexmedetomidine (0.1 mg/kg/hr, i.p.) and pancuronium (1 mg/kg/hr, i.p.), combined with low dose isoflurane at 0.5% to prevent epileptic activity². For drug infusion, an MR-compatible syringe pump must be used if the pump is to be placed in the magnetic environment. Alternatively, a noncompatible pump may be placed outside the magnetic environment provided that extended catheter tubing is used.

3. fMRI Data Acquisition

The third step is fMRI acquisition, including positioning, shimming, anatomical scans, and functional scans. A 9.4 Tesla system with a homemade surface coil is used here, though this technique may be adapted to other high-field systems and commercially made MRI coils.

1. Insert the rat into the scanner and position in the center of the magnet. Use a three-plane scout image to precisely center the rat within the magnet with respect to the brain regions of interest, and FASTMAP shimming to homogenize the magnetic field at the regions of interest.
2. Use a sagittal T2-weighted RARE sequence (FOV, 2.56 x 2.56 cm²; matrix size, 256 x 256; slice thickness, 1.5 mm; TR/TE, 1500/11 ms; RARE Factor, 8; Flip Angle, 180°) to find the location of the anterior commissure, and align the subsequent images to this location. Align eight-slice single-shot GE-EPI scans (FOV, 2.56 x 2.56 cm²; matrix size, 96 x 96, reconstructed to 128 x 128; slice thickness, 1mm; TR/TE, 1000/14 ms) to this point with coronal orientation.
3. For functional scans, use 70 consecutive EPI scans with 1 second temporal resolution synchronized to the stimulation output, set to 20 sec rest, 10 sec stimulation, followed by 40 sec rest. Allow a minimum of 90 sec between scans to allow for neurovascular recovery. Acquire multiple repeated scans at each stimulation parameter to improve the signal-to-noise ratio by averaging. Use a series of dummy scans (typically 4-8) immediately prior to scanning for noise reduction. Confirm the BOLD response at the time of image acquisition to ensure success of the experiment using the method described in section 4, though averaging, coregistration and skull-stripping may be skipped in this setting.
4. After functional scanning is complete, use a T2-weighted RARE spin-echo sequence (FOV, 2.56 x 2.56 cm²; matrix size, 256 x 256; slice thickness, 1 mm; TR/TE, 2500/33 ms; averages, 8) to measure the anatomical position of the electrode *in vivo*. Acquire multiple coronal and sagittal sections to measure the tip of the electrode artifact along anterior/posterior, medial/lateral and dorsal/ventral axes and confirm electrode placement. High resolution magnetic resonance microscopy (FOV, 1.8 x 1.28 cm; matrix size, 360 x 256; slice thickness, 0.5 mm; TR/TE, 2500/12.6 ms; RARE factor, 8; averages, 280) may be used to examine the precise location of the electrode tract after removal with respect to nearby neuroanatomical structures and confirm the accuracy of electrode placement³.

4. fMRI Data Processing and Analysis

The fourth step is processing and analysis of fMRI data, including generation of response maps and calculation of percent BOLD signal change. Custom programs running within a computing environment (e.g. MATLAB) or commercial fMRI software tools (e.g. SPM, FSL, or AFNI) may be employed.

1. Begin with image coregistration and averaging of data first within-subject by frequency, followed by across-subject. **Note:** We accomplish this using SPM codes.
2. Perform skull stripping to remove nonbrain tissue using manually defined region of interest (ROI) with signal thresholding. Automatic skull stripping algorithms may be employed.
3. Compile response maps by calculating the correlation coefficient of the relationship between BOLD response over time and the stimulation paradigm for each voxel. Delaying the paradigm several seconds to account for delay in hemodynamic response may be necessary. Set significant level at $P < 0.05$ after Bonferroni correction. Other statistical methods may be employed. Correcting for multiple comparisons using Random Field Theory or cluster-level correction based on Gaussian Random Field may be performed in place of the Bonferroni correction for more sensitive analysis⁴. **Note:** The hemodynamic delay may vary based on brain regions targeted, pharmacologic agents used, and physiological parameters. It is crucial to control these parameters in order to prevent variability within-subject and between-subjects.
4. Quantify the BOLD response by defining a ROI to extract time-course data. Average the percent signal change across all voxels within the same anatomical structure. Voxel-wise analysis using the General Linear Model may also be used⁵.

Representative Results

Representative functional data were acquired according to the above protocol in a single rat with a stimulating electrode implanted to the subthalamic nucleus on the right side. An illustration of essential setup for DBS fMRI image acquisition is provided in **Figure 1**. Stimulation was applied consistent with the above protocol, with an amplitude of 0.3 mA, frequency of 130 Hz and pulse width of 0.09 msec. Robust activation of ipsilateral motor cortex has been consistently visualized using this protocol with the subthalamic nucleus as the stimulation target. With a square-wave stimulation pattern, the BOLD signal would be expected to be modulated with respect to the baseline (no-stimulation condition) with a time course correlated to the stimulation period. Here positive BOLD responses are observed in the expected brain region (**Figure 2**) and with an ON/OFF pattern well-correlated to the stimulation paradigm, taking into account a brief hemodynamic delay (**Figure 3**). From the map (**Figure 2**), an overlaid neuroanatomical atlas¹ may be used to define precise regions of interest to compare the BOLD effect at individual brain regions. For STN DBS the BOLD response at the motor cortex is shown in **Figure 3**, though regions of interest may be placed in any brain area. These responses may then be averaged between scans and then between subjects to identify brain regions which produce a consistent response to stimulation. Targeting of other neuroanatomical structures may produce different response patterns than those shown in this experiment. Additionally, even a small degree of inaccuracy in electrode placement may produce large differences in response, as may differences in electrode types and electrical stimulation parameters³.

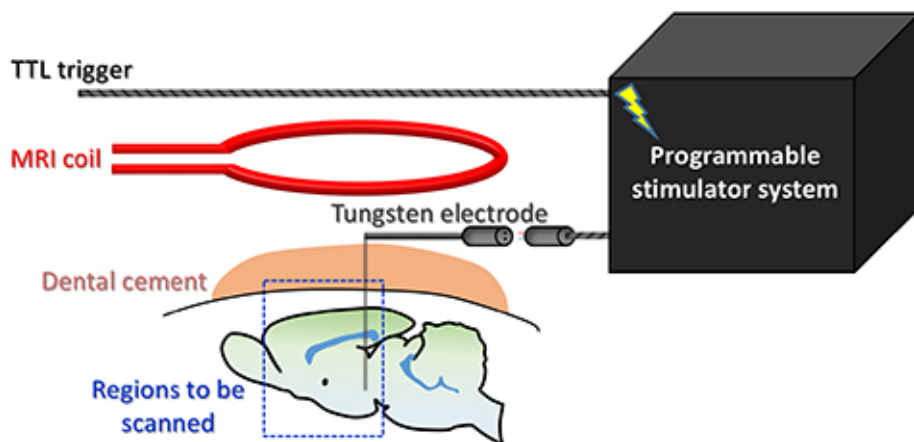


Figure 1. Scheme of basic fMRI configuration with surface coil, electrode position and stimulator synchronization.

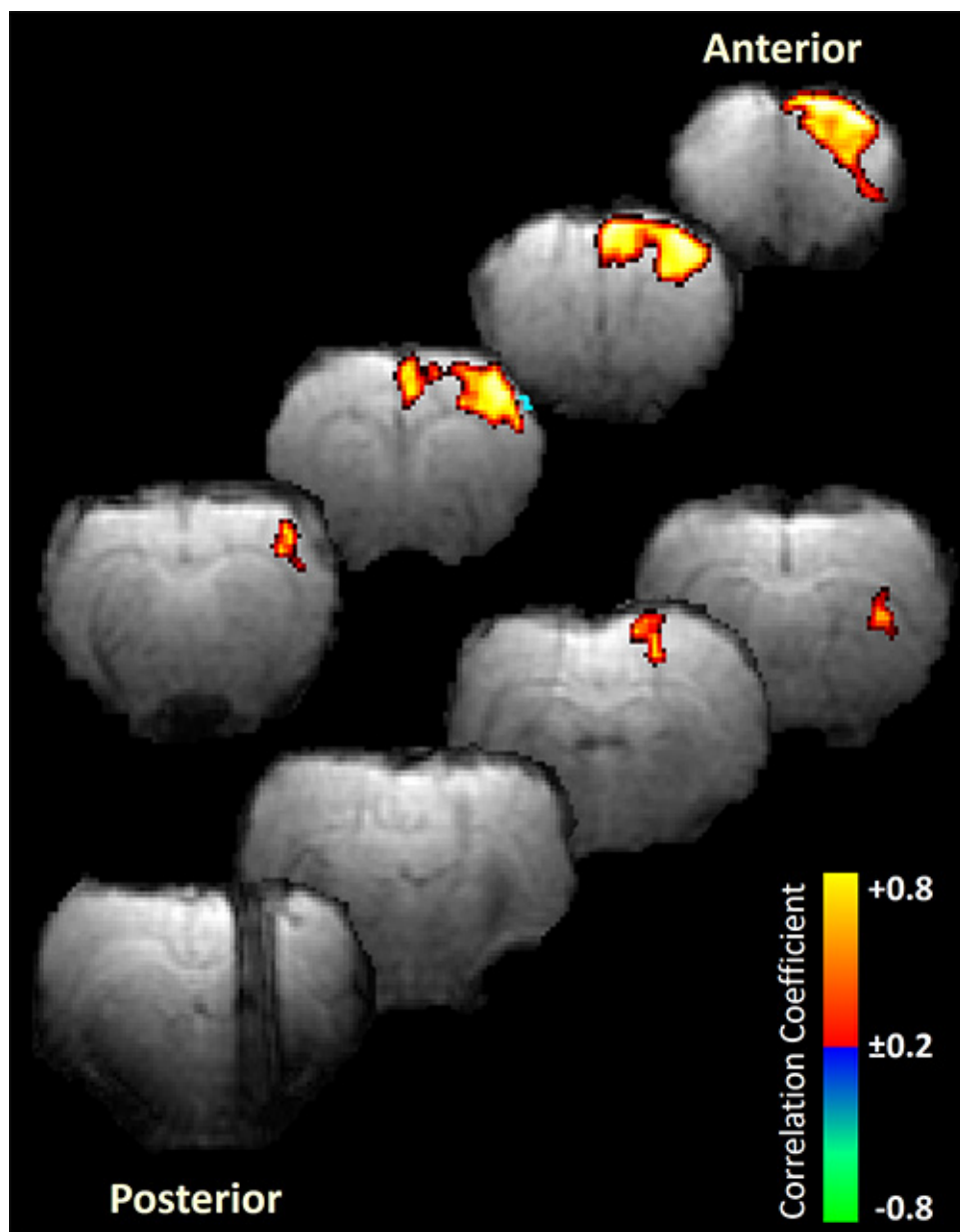


Figure 2. Representative EPI images labeled with correlation coefficients from a single animal, with posterior to anterior slices displayed left to right. Color bar indicates correlation coefficients at each voxel.

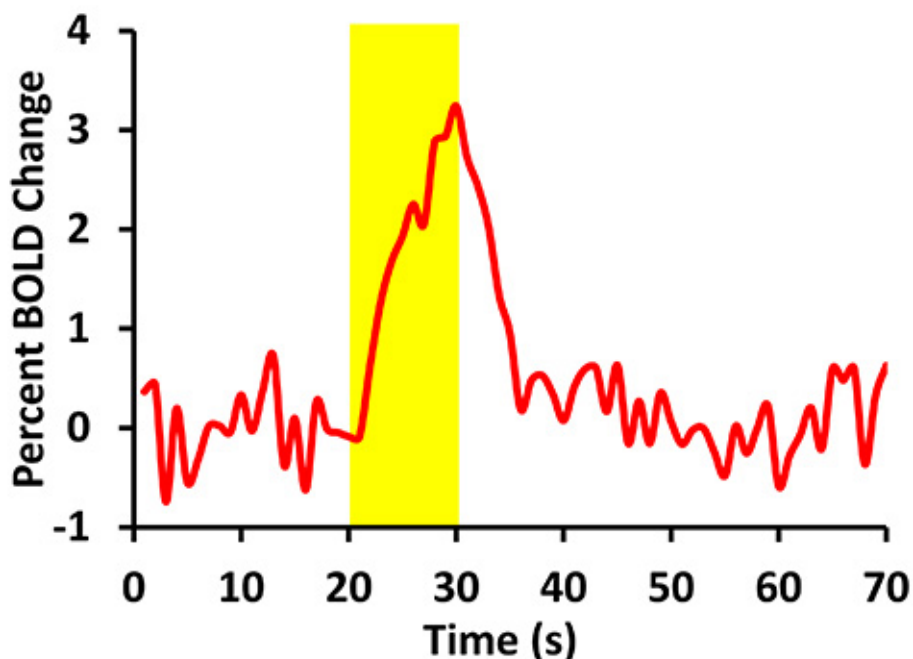


Figure 3. Typical % BOLD over time from a single animal averaged over multiple scans at the same stimulation parameters: 0.3 mA, 130 Hz, 0.09 msec pulse width. Yellow bar indicates period of time in which stimulation was applied to the subthalamic nucleus. ROI was within motor cortex. **Note:** These stimulation parameters are within the standard range for DBS at the STN, but may need to be modified for alternative stimulation sites.

Discussion

Simultaneous DBS and fMRI represents a promising experimental toolkit for the identification and characterization of global downstream responses to neural circuit stimulation, *in vivo*. The major advantage of this technique over other available tools, such as electrophysiological recordings, lies in the relatively unbiased nature of fMRI, whereby a large and diverse area of brain tissue can be examined for responsiveness to DBS at any target. Although the described protocol is specific for DBS-fMRI in the rat, neuroimaging of DBS responses has also been successfully conducted in other model organisms, including pigs⁶.

Perhaps the most obvious application for this technique is the modeling of DBS as applied therapeutically for certain neurological and psychiatric disorders, *i.e.* Parkinson's disease⁷⁻⁹. In Parkinson's disease patients, high frequency stimulation at either the subthalamic nucleus (STN) or internal globus pallidus (GPi) is effective for the alleviation of many motor symptoms¹⁰. High frequency DBS at either of these targets results in substantial activation within both canonical motor and limbic area^{8,6}. The characterization of these spatially dynamic fMRI responses, when complemented by behavioral analysis, may aid in the identification of therapeutic DBS circuits. The conclusions drawn from such studies should readily translate to the clinic, specifically for the refinement of DBS at existing targets and extension of DBS to new targets for various diseases and disorders.

General limitations of fMRI have been extensively reviewed elsewhere¹¹, although several specific limitations are particularly pertinent to DBS-fMRI. DBS may result in temporally dynamic changes in cellular activity¹² that may not be adequately resolved with fMRI. For experiments requiring finer temporal resolution than can currently be offered by fMRI alone, we suggest electrophysiological recordings, which may be acquired in conjunction with fMRI¹³⁻¹⁵. An additional issue concerns the complex BOLD responses observed in response to neural activity¹⁶⁻²¹. fMRI allows for the detection of areas modulated by DBS, although caution should be taken when inferring the direction of this modulation based on fMRI data alone. The application of multiple fMRI modalities (*e.g.* BOLD, cerebral blood flow, cerebral blood volume, functional connectivity, and manganese-enhanced MRI), as well as electrophysiological and histological data, should strengthen such conclusions.

Many of the details provided in this protocol can be readily adopted for alternative stimulation methods, including optogenetic targeting²². For optogenetic experiments, a laser driver can be interfaced with stimulation software to obtain TTL triggering of laser pulses. For such experiments, it is important to use a patch cable of appropriate length so that the optic fiber can be coupled to a laser driver located outside of the scanner room. Opto-fMRI allows for the detection of neurovascular changes induced by selective modulation of activity within genetically defined cell populations, while electrical DBS-fMRI responses cannot be easily attributed to recruitment of specific circuits. Nevertheless, electrical DBS is likely of greater translational value for studying therapeutic DBS, which solely relies on electrical stimulation in patient populations.

Concerns for safety and local tissue damage are important considerations for neuroimaging with simultaneous DBS in both clinical and animal research settings, and have been discussed extensively elsewhere (Carmichael^{23,24}). While many MRI sequences have the potential to cause significant heating and tissue damage, the stimulation parameters and scan sequences in this protocol are designed to minimize these factors,

particularly the length of each scan sequence between rest periods. As such, responses to stimulation after dozens of scans are consistently durable in pilot studies, and no signs of local tissue damage are seen on post-mortem imaging, confirming that this protocol is safe with regards to current delivery and MR compatibility of the electrode used.

The flexibility of the described DBS-fMRI procedure, coupled with the wealth of information provided regarding regional modulation profiles in response to DBS, make this procedure ideal for a variety of applications in systems-level neuroscience.

Disclosures

The authors have nothing to disclose.

Acknowledgements

We thank Shaili Jha and Heather Decot for assistance with filming.

References

1. Paxinos, G. & Watson, C. *The rat brain in stereotaxic coordinates, 5th edition*. Academic Press (2004).
2. Fukuda, M., Vazquez, A. L., Zong, X. & Kim, S. G. Effects of the alpha(2)-adrenergic receptor agonist dexmedetomidine on neural, vascular and BOLD fMRI responses in the somatosensory cortex. *Eur. J. Neurosci.* **37**, 80-95, doi:10.1111/ejn.12024 (2013).
3. Lai HY, Y. J., Albaugh DL, Kao YC, Shih YY. Functional MRI reveals frequency-dependent responses during deep brain stimulation at the subthalamic nucleus or internal globus pallidus. *NeuroImage. In press* (2013).
4. Brett M, W. D. P. a. S. K. in *Human Brain Function*. ed Richard S.J. Frackowiak and John T. Ashburner and William D. Penny and Semir Zeki. (2004).
5. Poline, J. B. & Brett, M. The general linear model and fMRI: does love last forever? *NeuroImage*. **62**, 871-880, doi:10.1016/j.neuroimage.2012.01.133 (2012).
6. Min, H. K. *et al.* Deep brain stimulation induces BOLD activation in motor and non-motor networks: an fMRI comparison study of STN and EN/GPi DBS in large animals. *NeuroImage*. **63**, 1408-1420, doi:10.1016/j.neuroimage.2012.08.006 (2012).
7. Lozano, Andres M. & Lipsman, N. Probing and Regulating Dysfunctional Circuits Using Deep Brain Stimulation. *Neuron*. **77**, 406-424, doi:10.1016/j.neuron.2013.01.020 (2013).
8. DeLong, M. & Wichmann, T. Deep brain stimulation for movement and other neurologic disorders. *Ann. N.Y. Acad. Sci.* **1265**, 1-8, doi:10.1111/j.1749-6632.2012.06608.x (2012).
9. Goodman, W. K. & Alterman, R. L. Deep brain stimulation for intractable psychiatric disorders. *Ann. Rev. Med.* **63**, 511-524, doi:10.1146/annurev-med-052209-100401 (2012).
10. Pizzolato, G. & Mandat, T. Deep brain stimulation for movement disorders. *Front. Integr. Neurosci.* **6**, 2, doi:10.3389/fnint.2012.00002 (2012).
11. Logothetis, N. K. What we can do and what we cannot do with fMRI. *Nature*. **453**, 869-878, doi:10.1038/nature06976 (2008).
12. Li, Q. *et al.* Therapeutic deep brain stimulation in Parkinsonian rats directly influences motor cortex. *Neuron*. **76**, 1030-1041, doi:10.1016/j.neuron.2012.09.032 (2012).
13. Pan, W., Thompson, G., Magnuson, M., Majeed, W., Jaeger, D., Keilholz, S. Simultaneous fMRI and Electrophysiology in the Rodent Brain. *J. Vis. Exp.* (42), e1901, doi:10.3791/1901 (2010).
14. Huttunen, J. K., Grohn, O. & Penttonen, M. Coupling between simultaneously recorded BOLD response and neuronal activity in the rat somatosensory cortex. *NeuroImage*. **39**, 775-785, doi:10.1016/j.neuroimage.2007.06.042 (2008).
15. Logothetis, N. K., Pauls, J., Augath, M., Trinath, T. & Oeltermann, A. Neurophysiological investigation of the basis of the fMRI signal. *Nature*. **412**, 150-157 (2001).
16. Shih, Y. Y. *et al.* A new scenario for negative functional magnetic resonance imaging signals: endogenous neurotransmission. *J. Neurosci.* **29**, 3036-3044, doi:10.1523/JNEUROSCI.3447-08.2009 (2009).
17. Shih, Y. Y., Wey, H. Y., De La Garza, B. H. & Duong, T. Q. Striatal and cortical BOLD, blood flow, blood volume, oxygen consumption, and glucose consumption changes in noxious forepaw electrical stimulation. *J. Cereb. Blood Flow Metab.* **31**, 832-841, doi:10.1038/jcbfm.2010.173 (2011).
18. Shmuel, A., Augath, M., Oeltermann, A. & Logothetis, N. K. Negative functional MRI response correlates with decreases in neuronal activity in monkey visual area V1. *Nat. Neurosci.* **9**, 569-577, doi:10.1038/nn1675 (2006).
19. Schridde, U. *et al.* Negative BOLD with large increases in neuronal activity. *Cereb. Cortex*. **18**, 1814-1827, doi:10.1093/cercor/bhm208 (2008).
20. Shmuel, A. *et al.* Sustained negative BOLD, blood flow and oxygen consumption response and its coupling to the positive response in the human brain. *Neuron*. **36**, 1195-1210 (2002).
21. Harel, N., Lee, S.-P., Nagaoka, T., Kim, D.-S. & Kim, S.-G. Origin of negative blood oxygenation level-dependent fMRI signals. *J. Cereb. Blood Flow Metab.* **22**, 908-917 (2002).
22. Lee, J. H. *et al.* Global and local fMRI signals driven by neurons defined optogenetically by type and wiring. *Nature*. **465**, 788-792, doi:10.1038/nature09108 (2010).
23. Carmichael, D. W. *et al.* Functional MRI with active, fully implanted, deep brain stimulation systems: safety and experimental confounds. *NeuroImage*. **37**, 508-517, doi:10.1016/j.neuroimage.2007.04.058 (2007).
24. Tagliati, M. *et al.* Safety of MRI in patients with implanted deep brain stimulation devices. *NeuroImage*. **47 Suppl 2**, T53-57, doi:10.1016/j.neuroimage.2009.04.044 (2009).